Isotactic Polypropylene Composites Reinforced with Multiwall Carbon Nanotubes, Part 2: Thermal and Mechanical Properties Related to the Structure

Rumiana Kotsilkova,[1] Evgeni Ivanov,[1] Ekaterina Krusteva,[1] Clara Silvestre,[2] Sossio Cimmino,[2] Donatella Duraccio[2]

[1]*Central Lab Physico-Chemical Mechanics, Bulgarian Academy of Sciences, Sofia, Bulgaria*
[2]*Institute of Chemistry and Technology of Polymers, CNR. Via Campi Flegrei 34, Pozzuoli 80078, NA, Italy*

Received 27 December 2008; accepted 16 March 2009
DOI 10.1002/app.30413
Published online 4 November 2009 in Wiley InterScience (www.interscience.wiley.com).

ABSTRACT: Polypropylene nanocomposites containing multiwall carbon nanotubes (MWCNT), from 0.1 to 3 wt %, are prepared by dilution of a polypropylene based masterbatch (20% MWCNT) with isotactic polypropylene (iPP) using extrusion processing. CNT are found to enhance significantly the thermal stability of iPP in nitrogen and air atmosphere. Dynamic mechanical analysis and tensile tests confirm the reinforcement effect of small amount of nanotubes in iPP. Rheology, structure, and properties are correlated determine the optimal limits of nanofiller content required for improving the performance of nanocomposites. The rheological flocculation threshold of $\varphi^* = 0.5\%$ is found as a critical concentration for the formation of a flocculated type of structure in the dispersions. It is proposed, that the flocculated structure is responsible for the maximal improvement of nanocomposite mechanical and thermal properties. The MWCNT additive slightly enhances the local dynamics of iPP molecules in the glass transition region and suppresses the global relaxation of the chain segments in the amorphous regions, resulting in a reinforcement effect. The fracture mechanism is discussed and associated with the hierarchy of the flocculated nanocomposite morphology and the bridging of matrix cracks by CNT. © 2009 Wiley Periodicals, Inc. J Appl Polym Sci 115: 3576–3585, 2010

Key words: polypropylene nanocomposites; carbon nanotubes; thermal stability; dynamic mechanical properties; tensile characteristics; rheology-structure-property relations; reinforcement

INTRODUCTION

Recently, polymer/carbon nanotube composites have gained intensive interest, as carbon nanotubes (CNT) have a high potential to improve the mechanical and thermal properties of polymers.[1–4] CNT exhibit exceptionally high aspect ratio in combination with unique mechanical, thermal, and electronic properties,[5–7] which make them a potential candidate for the reinforcement of polymers. However, the key point is to transfer the extraordinary properties of CNT to the polymer composite. This may be achieved by their uniform dispersion, exfoliation, and orientation in the polymeric matrix, as well as by the interaction between CNT and the polymer matrix, which is also important.

A lot of studies reported that the introduction of nanoparticles and particularly of CNT in the polymer matrices may improve their applications in the field of reinforcing composites.[8–12] New combinations of properties that ensue from the nanoscale structure of polymer nanocomposites provide opportunities to outperform conventional reinforced plastics, thus enhancing the promise of nanoengineered materials applications. The huge potential of CNTs for the improvement of the fracture mechanical performance of polymer composites was highlighted at low filler contents. The dispersion of nanotubes in the matrix polymer and the control of nanotube interactions are found to be a challenge to overcome for nanotube-reinforced polymers.[8]

In our previous studies, we have determined two critical concentrations (rheological thresholds) presenting the structural transitions in nanodispersions, as varying the nanofiller content.[9–11] The first rheological threshold was related to the formation of a dispersion structure dominated by flocs, and it was called "rheological flocculation threshold" (or "mechanical percolation"). The second rheological threshold was related with formation of a network (gel-like) structure of nanofiller in the matrix polymer, the so called "rheological percolation threshold." Moreover, a strong corelation between the

Correspondence to: R. Kotsilkova (kotsilkova@yahoo.com).
Contract grant sponsors: Bilateral Project CLPCM-BAS, Bulgaria/ICTP-CNR, Italy; the FP7-CSA-NaPolyNet; the NT4-02-D01-469/06, NSF-BG; and D-02-53/08, NSF-BG.

rheological thresholds and the properties improvement of polymer nanocomposites was observed. This rheology-structure-property relationship was proposed to be a basis for the design of nanocomposites with controlled structure and predictable properties improvements.

Recently, isotactic polypropylene (iPP) nanocomposites with CNT have been intensively studied.[13–15] Dynamic mechanical properties, tensile strength and modulus of the melt-spun iPP fibrils were found to be increased. Moreover, nanotubes enhance the thermal stability and flammability of iPP. A largely improved ductility of PP/multiwall carbon nanotubes (MWCNT) composites was achieved via dynamic packaging injection molding.[16] A lot of the reports stress on the preparation and properties of nanocomposites.[9–11,17] In most cases, compatibilizers or coupling agents are used to modify polypropylene or filler additives because of weak interaction.

In this article, we prove the aforementioned concept of rheology-structure-property relationship for the design of polypropylene/carbon nanotube composites with enhanced thermal and mechanical properties. The main goal of this study is to analyze the thermal and mechanical properties improvements of polypropylene nanocomposites, prepared by using a commercial masterbatch of MWCNT in polypropylene. To investigate the miscibility of this masterbatch in iPP, the compositions are prepared without using compaibilisers, thus relying on the effects of the coupling agents contained in the masterbatch. Corelations between the first rheological threshold (flocculation threshold), the structure and mechanical and thermal properties improvement of iPP/MWCNT composites are discussed providing a concept for the reinforcement mechanism.

EXPERIMENTAL

A commercial masterbatch containing 20% MWCNT in polypropylene is supplied by Hyperion Catalysis Int. The masterbatch contains initially dispersed intertwined agglomerates of parallel, MWCNT, commercially manufactured from high purity, low molecular weight hydrocarbons in a continuous, gas phase catalyzed reaction. Typical outside diameter range of the nanotube is from 10 to 15 nm, the length is between 1 and 10 μm, and the density is $\sim$1.75 g/cm^3. The commercial masterbatch contains appropriate coupling agents, which are used to assist the dispersion of CNT in polypropylene (Hyperion).

To prepare nanocomposites, the commercial masterbatch was let down with iPP "Buplen 6231" with a density, $\rho = 901$ kg/m^3 and a zero shear viscosity, $\eta_o = 200$ Pa s (at 190°C), this supplied by Lukoil Neftochim Co., Bulgaria. The iPP/MWCNTs composites were produced by direct melt compounding in Brabender DSE 35/17D twin screw extruder with a screw speed of 30 rpm and melt temperature of 200°C, according to a two-step process. The compositions were extruded in 3 runs and further calendered as sheets with thickness of about of 1.5 mm under the same temperature conditions. In this study, well homogenized test specimens taken after the third extrusion run were punched from the sheets for further characterization. Compounds of iPP/MWCNTs composites of different carbon nanotube concentrations (0, 0.1, 0.5, 1, 2, and 3 wt %) were produced without using compatibiliser. We apply this processing approach to investigate the effects of the coupling agents, contained in the commercial masterbatch, on the miscibility with iPP.

Thermal gravimetric analyses (TGA) were conducted using a Diamond Perkin-Elmer Instrument (TG/DTA) at 5°C/min and 20°C/min from 25°C to 800°C in nitrogen and air atmosphere. The samples (ca. 5 mg) were placed in open ceramic pans.

Dynamic-mechanical data were collected at a frequency of 1 Hz and at a heating rate of 4°C/min within the temperature range from −100°C to 120°C in nitrogen atmosphere, using DMTA III Polymer Laboratories in banding mode. Samples with size of 50 × 8 × 1 mm were used.

The tensile experiments were carried out with the "Tiratest 2300" universal testing machine. The oriented direction of the MWCNT during calender processing is parallel to tensile deformation direction. The moving speed of the crosshead was 10 mm/min for the tensile measurements and the ambient temperature was 20°C. Standard test specimens with size of 100 × 8 × 1 mm were used. The values of the tensile characteristics were calculated as the average over six samples for each composition.

Morphology of the bulk is studied by scanning electron microscopy (SEM), using JEM 2CX (Joel), with resolution of 40Å and accelerated voltage of 100 kV. Samples are cut in liquid nitrogen and covered with vacuum evaporated carbon and gold. The hierarchy of the nanocomposite structure is estimated at different magnification within the range from 100 to 0.2 μm.

RESULTS AND DISCUSSION

Thermal properties in nitrogen and air atmosphere

TGA and corresponding DTG results of iPP and nanocomposites containing 1%, 2%, and 3% MWCNT are reported here in both nitrogen and air atmosphere at heating rates of 5°C/min and 20°C/min, respectively. In Table I, we compare two degradation temperatures: (i) the peak temperature (T_p)

TABLE I
DTG Peak Temperature (T_p) and TGA Decomposition Temperature at 10% Weight Loss ($T_{0.1}$) in Nitrogen and Air Atmosphere

	N_2				AIR			
	5°C/min		20°C/min		5°C/min		20°C/min	
	$T_{0.1}$ (°C)	T_p (°C)	$T_{0.1}$ (°C)	T_p (°C)	$T_{0.1}$ (°C)	T_p (°C)	$T_{0.1}$ (°C)	T_p (°C)
iPP	415	445	433	467	246	297	297	390
1% MWCNT	426	447	450	475	254	344	305	406
2% MWCNT	430	450	454	476	266	370	310	400–414
3% MWCNT	432	451	456	478	268	378	313	417

on the DTG curves, representing the temperature at which the maximum weight loss rate is reached; and (ii) the temperature ($T_{0.1}$) of decomposition at which the weight loss is 10%, as determined under the aforementioned test conditions.

Figure 1 reports the TGA curves, presenting the relative weight loss vs. temperature [Fig. 1(a,c)], and the first derivative (DTG) of the TGA curves [Fig. 1(b,d)] in nitrogen atmosphere at 5°C/min [Fig. 1(a,b)] and 20°C/min [Fig. 1(c,d)]. The results obtained with both heating rates in nitrogen atmosphere were qualitatively similar. The difference is that the curves at 20°C/min are shifted toward higher temperatures compared with the curves at 5°C/min. The iPP degrades with a single step corresponding to the thermal degradation of iPP initiated primarily by thermal scissions of C—C chain bonds accompanied by a transfer of hydrogen at the site scission.[18] Generally, the addition of nanotubes in the investigated concentration range enhances the thermal stability of iPP in nitrogen atmosphere. Importantly, a significant improvement of thermal properties appears at the low filler content of 1%, where the TGA curves of iPP/MWCNT composites are shifted significantly toward higher temperatures, as compared with iPP. However, further increase of the nanotube amount (up to 3%) does not make a strong enhancement in thermal stability of the nanocomposite systems. An example in Table I shows, that the $T_{0.1}$ of composites with 1%–3% MWCNT is

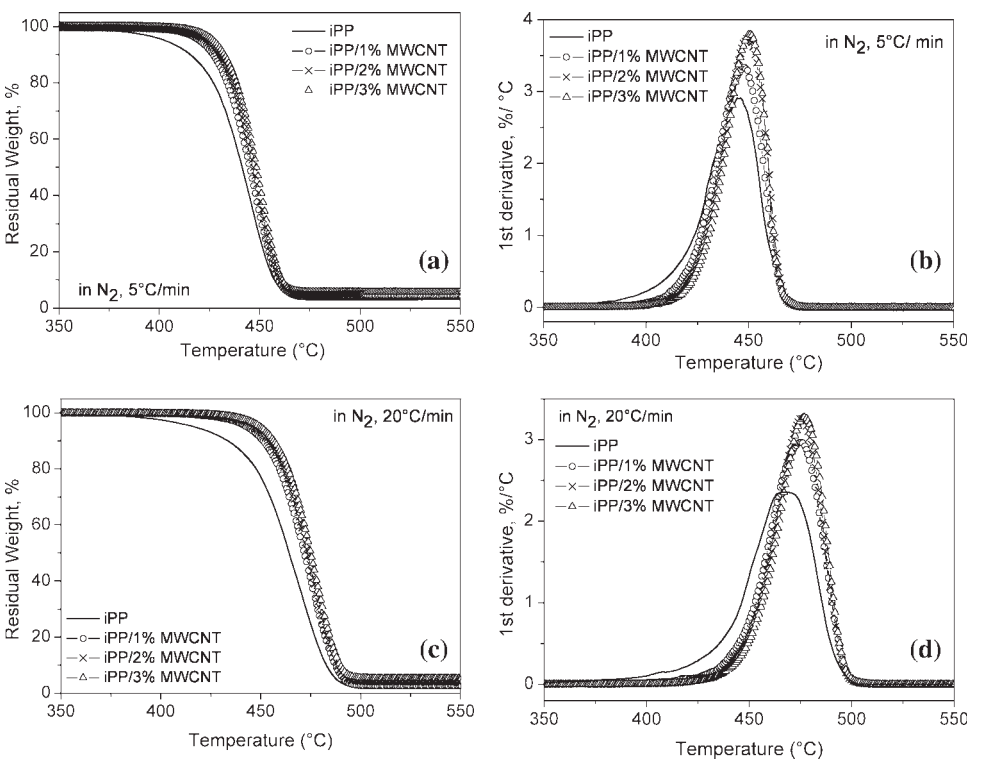

Figure 1 TGA curves (residual weight vs. temperature) and the corresponding first derivative (DTG curves) in nitrogen atmosphere. Data for iPP and nanocomposites with 1%, 2%, and 3% MWCNT at two heating rates are presented: (a, b) 5°C/min and (c, d) 20°C/min.

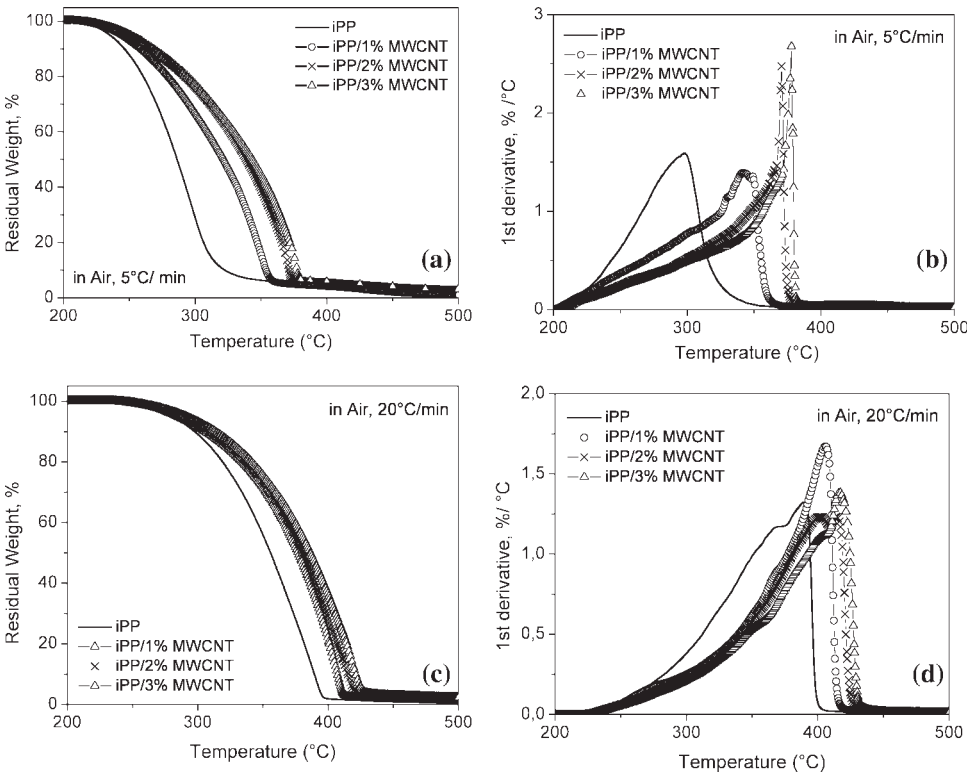

Figure 2 TGA curves (residual weight vs. temperature) and the corresponding first derivative (DTG) in air atmosphere. Data for iPP and nanocomposites with 1%, 2%, and 3% MWCNT at two heating rates are compared: (a, b) 5°C/min and (c, d) 20°C/min.

shifted with 17°C–23°C toward higher temperatures, as well as the T_p is increased with 8°C–11 °C at a heating rate of 20°C/min, as compared to the pristine polymer.

Thermal degradation of the samples in air atmosphere is significantly different from that in nitrogen. Moreover, the results obtained at the heating rate of 5°C/min presented a higher effect of nanotube additive on the iPP thermal degradation, compared with those at 20°C/min. Example TGA and DTG results in air at both heating rates of 5°C/min and 20°C/min are plotted in Figure 2(a–d). Table I presents in details the degradation temperatures in air atmosphere for both heating rates. The DTG curve of iPP obtained at the heating rate of 5°C/min, shows a broad mass rate peak centred at about $T_p = 297$°C in air [Fig. 2(b)], compared with $T_p = 440$°C in nitrogen [Fig. 1(b)]; thus, the thermal stability of iPP is prominently reduced by oxidative dehydrogenation accompanied by hydrogen abstraction.[19] The iPP/MWCNT nanocomposites are more stable than iPP in air atmosphere. For example the $T_{0.1}$ of 1%–3% iPP/MWCNT composites increases with 8°C–20°C, as well as very large is the increase of T_p (with 47°C–81°C), as compared with the pristine polymer. Particularly, the nanocomposites present a complex thermal degradation in air atmosphere (visible in DTG curves at 5°C/min) [Fig. 2(b)]. This could be caused by a small amount of iron in the MWCNT. It is reported that iron particles are formed from ferrocene used as catalyst to make MWCNT.[20] Iron is pyrophoric and could reduce the thermal oxidative stability of MWCNT, acting as catalyst during the oxidative degradation of the iPP/MWNT nanocomposites.

All the results indicate that the addition of nanotubes significantly enhances the thermal stability of iPP in both nitrogen and air atmosphere. This effect could be attributed to two different reasons. The first one considers a barrier labyrinth effect of nanotubes so that the diffusion of degradation products from the bulk of the polymer to the gas phase is slowed down. The second reason is a strong adsorption of iPP molecules on the nanotube surfaces.[21] We believe that in our case, the reason for the thermal properties improvement is the dispersion structure of interconnected nanotubes (flocs), which attract large amount of iPP molecules physically adsorbed on the nanotube surface within the flocks. These molecules are much less active than those in the volume and far from the nanotubes surfaces, thus their volatilization is delayed as evidenced by the peak temperature increase.

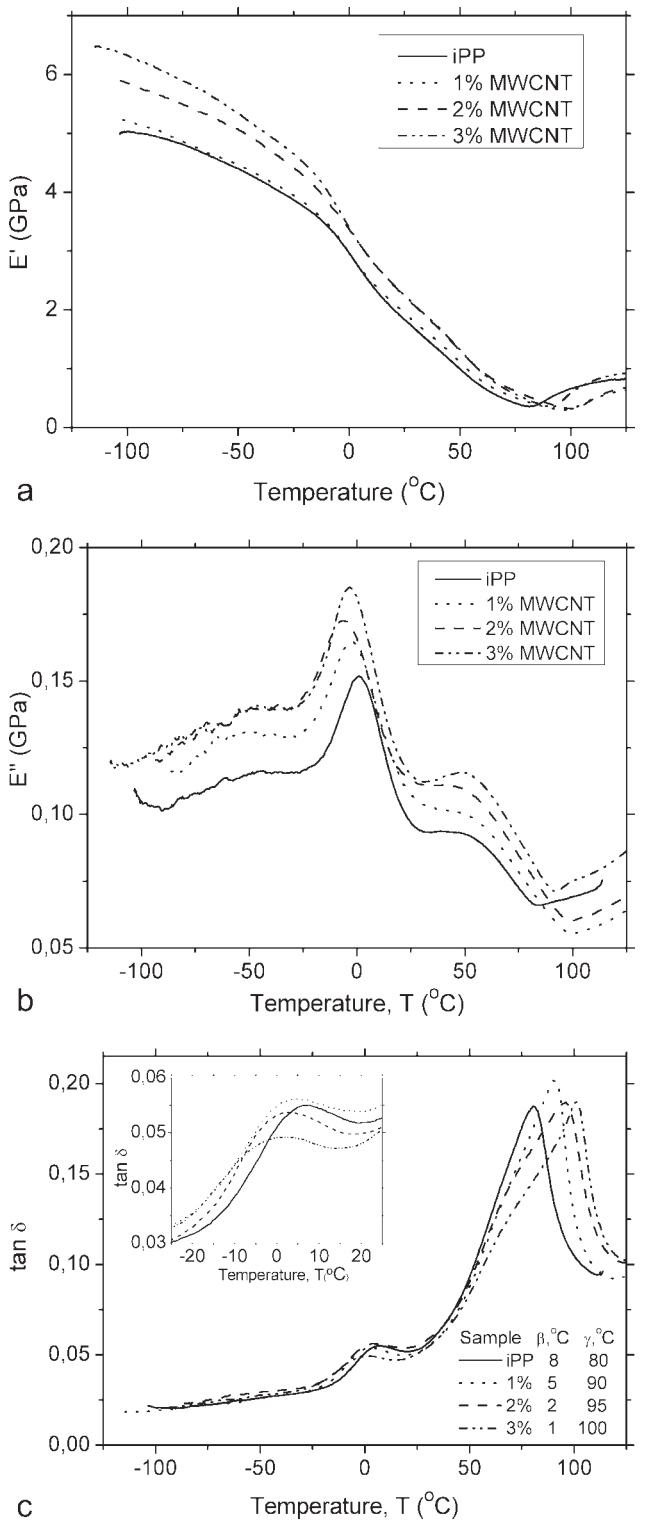

Figure 3 (a) Storage modulus (E'), (b) loss modulus (E''), and (c) loss tangent (tan $\delta = E''/E'$) vs. temperature of iPP and nanocomposites containing 1%, 2%, and 3% MWCNT, at frequency of 1Hz. The intercept in c represents the glass transition region. The values of β and γ-relaxation peaks are listed in c.

Dynamic mechanical properties

Dynamic mechanical properties, storage modulus (E'), loss modulus (E''), and loss tangent (tan δ), vs. temperature in the range of −110°C to 120°C are presented in Figure 3(a–c) for iPP and composites containing 1%, 2%, and 3% MWCNT. In Figure 3(a) we observe, that E' of the sample containing 1% MWCNT is similar to that of the matrix iPP. However, an improvement of about 30% of the tensile storage modulus in the glassy region is observed for 3% iPP/MWCNT composites compared with the polypropylene. Thus, E' reaches values of 5.8 and 6.5 GPa for 2% and 3% MWCNT composites, respectively, compared with 5 GPa for the pristine iPP at a temperature of −100°C. Such an increase of the storage modulus with increasing the nanotube content represents the contribution of the nanotubes on the overall modulus of nanocomposites. This contribution is high due to the exceptionally high Young's moduli of MWCNTs (in the terapascal range), the interfacial interactions, and the large aspect ratio of nanotubes producing interconnectivity at these filler contents. As the storage modulus E' reflects the elastic properties of the material, these results indicate reinforcement of nanocomposites and enhancement of stiffness.

The loss modulus, E'' in Figure 3(b) and, particularly, the loss factor tan δ ($= E''/E'$) in Figure 3(c) are very sensitive to the structural transformation of the material produced on increasing the temperature and provide a very efficient means of analysis in the timescale of the relaxation. As pointed in some investigations,[22] the tan δ curve of polypropylene shows three relaxations. The α-relaxation is attributed to the lamellar slip and rotation in the crystalline phase; the β-relaxation represents the dynamic glass transition; and the γ-peak is generally attributed to the relaxation of a few chain segments in the amorphous regions of the semicrystalline polymer. In our systems, both E'' and tan δ curves show the β and γ-relaxation peaks of the pristine iPP and the nanocomposites containing 1%–3% MWCNT. The large peak of E'' [Fig. 3(b)] and an intercept in Figure 3(c) of the tan δ curve present more details on the β-relaxation peak, which shows a dynamic glass transition at about 8°C for the pristine iPP, followed by a slight decrease in the order of 5°C, 2°C, and 1°C for the composites of 1%, 2%, and 3% MWCNT, respectively.

Such a slight decrease in the β-peak temperature indicates an enhancement of the local dynamics of iPP molecules in the glass transition region by the presence of CNT. A similar increase in local chain mobility due to the incorporation of nanoparticles has been found in other nanocomposites (e.g., polyimide/silica nanocomposites[23,24] and epoxy/smectite nanocomposites[9,10]) by molecular dynamic studies using dielectric techniques. A possible explanation for this increase in local mobility is that confinement of the polymer in nanoscale spaces between the nanoparticles and strong polymer–particle

interactions cause loosened molecular packing of polymeric chains and increased free volume in the composites with respect to the pure matrix.

As seen in Figure 3(b) the position of the γ-peak remains unchanged in the E'' plots. However, the values of the loss modulus increase strongly by increasing the nanotube contents in the range of both peaks. This suggests suppression of overall dynamics of iPP molecules by the presence of nanotubes, related to surface–polymer interactions. The γ-relaxation peak of the tan δ plot in Figure 3(c) is shifted towards higher temperatures by addition of nanotubes, probably due to the rapid decrease of E' in the region of the gamma peak. The magnitude of tan δ around the γ-peak is slightly higher or similar to that of the control polypropylene and the broadness of the peak is not influenced by the presence of nanotubes.

Semicrystalline polymers, which contain both crystalline and amorphous components, reveal more complex microstructures, with an amorphous phase between the crystalline lamellae, and with most of the macromolecular chains penetrating into both phases.[25] Therefore, both the increase of the γ-relaxation peak temperature of the tan δ, and the increased values of E″ of nanocomposites, compared to pristine polymer, may be related with cohesive interactions between the large surface area of nanotubes and amorphous iPP components. The absorbed polymer segments are less mobile than those in the volume. This results in suppression of the global relaxation of the chain segments in the amorphous regions, leading to enhancement of the viscoelastic properties of polymer nanocomposites.

Enhancement in tensile properties

The typical stress-strain curves of iPP and composites, with varying the MWCNT content from 0.1%–3%, are shown in Figure 4. The fracture mode of iPP is brittle, with elongation less than 10%. The produced composites exhibit an increase in tensile stress by adding MWCNT, but the strain at break decreases compared with that of the pristine polymer. Moreover, these effects depend significantly on the nanotube content. The highest increase of the strength at a relatively low decrease of elongation is observed at very low nanotube content (up to 0.5% MWCNT).

Further on, in Figure 5 are plotted the average values of the tensile strength [Fig. 5(a)], the Young's modulus [Fig. 5(b)] and the elongation [Fig. 5(c)], vs. nanotube content, using data from the Figure 4. We observed a maximum enhancement of the tensile strength ~15% by adding of small amount of 0.1%–0.5% MWCN to the iPP matrix. With nanotube content above 0.5%, the values of the tensile strength sharply decrease below that of the pristine polymer. The tensile modulus (Young's modulus) demonstrates also a maximum enhancement (~23%) at the same low nanotube content as the tensile strength, reaching values of 1.85 GPa (at 0.5% MWCNT) compared with 1.5 GPa of pristine iPP. However, the elongation to break decreases significantly with increasing the nanotube content. Therefore, the reinforcement effect of CNT on iPP is related mostly with enhanced stiffness, but the elasticity is decreased.

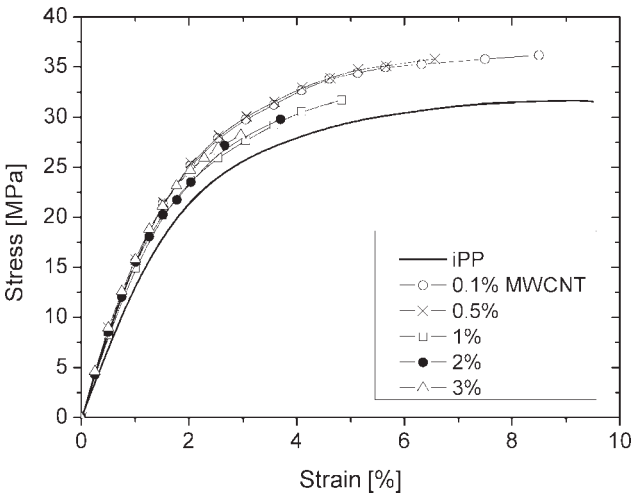

Figure 4 Stress-strain behavior of iPP and composites containing 0.1%, 0.5%, 1%, 2%, and 3% MWCNT. The tests velocity is 10 mm/min.

Importantly, the statistic deviation of the reported data becomes relatively high by increasing the nanotube content above 0.5%. This confirms our previous rheological results,[9–11] proposing that around the rheological flocculation threshold the polymer is intercalated between nanotubes into bundles and they can be desegregated. This results in a homogeneous dispersion. However, at higher nanofiller content, the large quantity of nanotubes does not allow the intercalation of a large quantity of polymer between MWCNT into bundles, this resulting in aggravation of homogeneity of the dispersions.

Mechanism of the reinforcement and rheology-structure-property relationship

There is clear evidence, that the main fracture mechanical mechanism in polymer nanocomposites is related to the enormous surface area of nanofillers in general.[1,8] However, two main aspects have to be considered in the as-prepared iPP composites, when the nanotube content increases. These are (i) the structure of dispersed nanotubes, formed in the iPP matrix and (ii) the homogeneity of the systems.

As discussed in our previous investigations,[9–11] the transition from a dispersed structure of single nanofillers to a flocculated structure of interconnected nanofillers in polymer nanocomposites

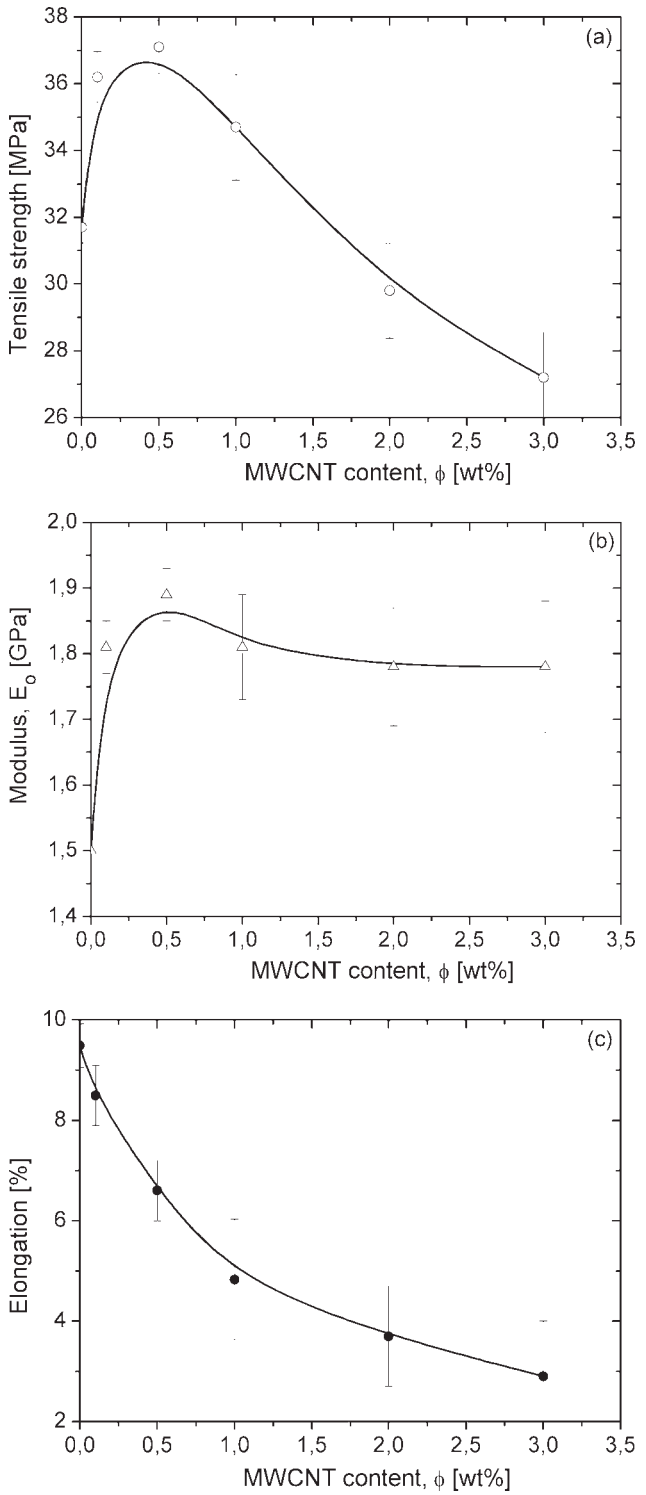

Figure 5 Tesile strength (a), Young's modulus (b), and the elongation at break (c), as functions of carbon nanotube content. Data from this figure are used.

appears around the rheological flocculation threshold, φ*. Importantly, the floccules incorporate a large amount of the matrix polymer, absorbed on the nanofiller surface. The dispersion structure of individual flocs around φ* determines the main fracture mechanism at these filler contents, which is defined as void nucleation and crack deflection localized at the floccules.[1,9] In fundamental aspect, the flocculated structure is expected to produce a significant growth of the process zone in front of the crack tip due to the stress strain interaction between the nanotubes and the matrix.[11] We apply such approach to relate the structure and mechanical properties, when discuss the role of carbon nanotube additive on the performance of iPP/MWCNT composites.

To explain the fundamental importance of the dispersion structure around the rheological flocculation threshold, we discuss the rheology-structure-property relationship in iPP/MWCNT composites. Figure 6 presents the normalized values (X/Xo), where the example characteristic of the nanocomposite (X) is divided to the corresponding characteristic of the pure iPP (X_o), plotted as a function of nanotube content. The following relative characteristics are compared: the dynamic viscosity at $\omega = 75\ s^{-1}$ (η/η_o); the DMTA storage modulus at −100°C (E'/E'_o); the DTG peak at 5°C/min in air ($T_p/T_{p,o}$); the Young's modulus (E/E_o); and the tensile strength (σ/σ_o). The arrow points the rheological flocculation threshold, $\varphi^* = 0.5\%$, determined from the viscosity curve, using an approach proposed in our previous investigations.[9]

As seen from the correlations in Figure 6, the maximum enhancement of the tensile strength and modulus is observed around the rheological flocculation threshold of $\varphi^* = 0.5\%$. A sharp increase in the dynamic storage modulus is observed above φ*. These properties improvements correlate well with the formation of a flocculated structure of interconnected nanotubes, which attract a large amount of iPP molecules adsorbed at the nanotube surface.

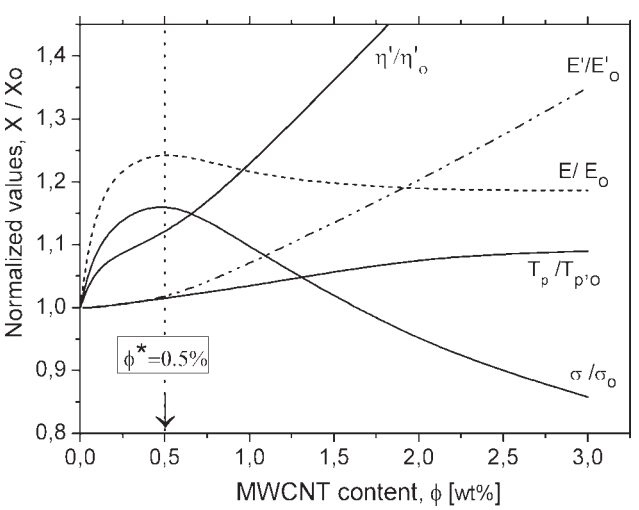

Figure 6 Normalized values of dynamic viscosity, storage modulus (at −100°C), DTG peak (at 5°C/min in air), Young's modulus, and tensile strength, as functions of carbon nanotube content. The arrow points at the rheological flocculation threshold, $\varphi^* = 0.5\%$.

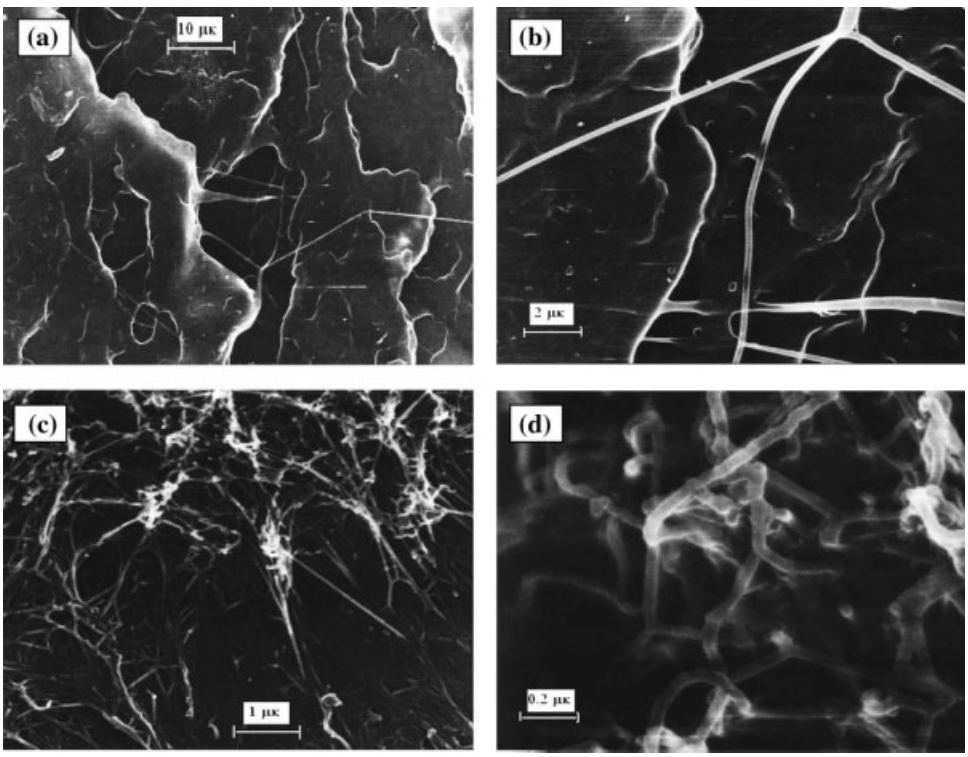

Figure 7 SEM micrographs of 0.5% iPP/MWCNT composite at different magnification: (a) 10 μm; (b) 2 μm; (c) 1 μm; (d) 0.2 μm.

Importantly, the increase of the nanotube content above the rheological flocculation threshold produces a strong decrease of the relative tensile characteristics, shown in Figure 6. We attribute these observations to the worsening of the homogeneity of the dispersions at higher nanotube contents. Obviously, the homogeneous distribution of the nanotubes in the matrix and the limited amount of individual floccules around φ* are responsible for the enhancement in fracture toughness. On the other side, the elastic modulus enhancement, as well as the maximal thermal properties improvement is reached at higher nanotube contents, above φ*. We relate these results to the physical absorption of a large amount of iPP molecules on the nanotube surface and formation of a network structure of interconnected flocs.

All observations above are very important for establishing the rheology-structure-property relationship for iPP/MWCNT composites as a novel design approach. The rheological flocculation threshold may be proposed as a prognostic concentration limit of nanotubes to optimize nanocomposite structure, which produces mechanical and thermal properties enhancement. Such a design approach is proved in our previous studies on variety of polymer nanocomposites.[9–11]

Scanning electron microscopy (SEM) (Figs. 7–9) is used for visualization of the morphology of nanocomposites, as well as for confirming the structure-property relationships. The hierarchy of the nanocomposite morphology is an important factor for understanding the reinforcement effects of the carbon nanotube dispersion structure in the iPP matrix. Hence, Figure 7 demonstrates the hierarchy of the nanocomposite structure by increased magnification of the SEM images for an example iPP/MWCNT sample. Here, the nanotube content coincides with the rheological flocculation threshold of $\varphi^* = 0.5\%$. In Figure 7(a), a good quality of the dispersion of nanotubes in iPP can be seen at large scales (a low magnification). By increasing the magnification, Figure 7(b), one can see a few well dispersed MWCNT with a large aspect ratio. Although, in another local place of the sample, Figure 7(c), a structure of fractal floccules is observed, which incorporate nanotubes and matrix polymer. At the highest magnification, Figure 7(d) demonstrates that the floccules are penetrated by the iPP matrix.

Figure 8 examines the fracture surface of the pristine polymer and nanocomposite samples. As seen in Figure 8(a), the surface of the pure iPP is smooth at 1-μm magnification, confirming the brittle fracture mode. For the 0.1% MWCNT composite, Figure 8(b), the fracture surface represents an absolutely different morphology on the same large scale (1 μm), which is rugged and the distorted matrix is observed. This indicates a different fracture

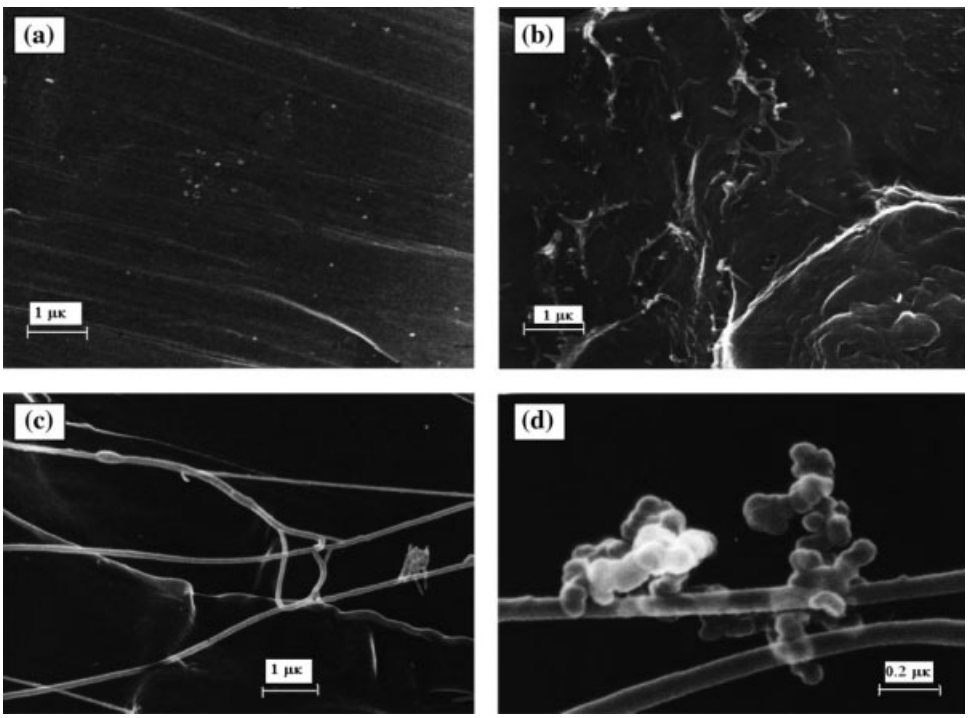

Figure 8 SEM images of the fracture surface of: (a) pure iPP; (b) iPP/0.1% MWCNT; and (c) iPP/1% MWCNT with magnification 1 μm; and (d) iPP/1% MWCNT with magnification 0.2 μm.

mechanism produced by the presence of CNT in the matrix polymer. At a high nanotube content of 1%, in Figure 8(c), the alignment of MWCNT along the processing direction (calendering) is clearly observed at magnification of 1 μm. On a larger magnification of 0.2 μm, a complex structure is visible in Figure 8(d) for the same 1% MWCNT composite, which consists of long nanotubes and particle-like aggregates, these are probably introduced in iPP by the masterbatch.

Figure 9 shows SEM micrographs of 1% and 0.1% MWCNT composites at different magnifications, presenting single fibrils, which are bridged to the iPP matrix. Moreover, the bridged fibrils are oriented perpendicularly to the crack front. Therefore, the positive influence of the CNT on the fracture mechanism can be related with bridging a matrix crack. As seen in Figure 9(a) for 1% MWCNT composites at low magnification (10 μm), the nanotubes are bended because of the translational movement of the crack front. Another example for the capability of CNT to bridge cracks is shown in Figure 9(b) for 0.1% MWCNT composite at a high magnification (0.2 μm). The SEM micrograph is focused inside the matrix crack, and a few nanotubes can be observed bridging cracks. Again the stressed fibrils are oriented perpendicularly to the crack surface, meaning that they carry tensile loads. Similar results are reported for epoxy nanocomposites containing double wall CNT.[8]

CONCLUSIONS

This study reports on the enhanced thermal and mechanical properties of the nanocomposites prepared by diluting a polypropylene based MWCNT masterbatch with iPP. To explain the fundamental importance of the dispersion structure of nanotubes, we apply the rheology-structure-property relationship as a novel design approach for the iPP/MWCNT composites. We relate the rheological flocculation threshold (φ^*) with the improvement of the thermal and mechanical properties of nanocomposites, and these correlations are explained with the effects of the flocculated type nanostructure of composites.

Two main aspects are considered to be dominant for the mechanical and thermal properties improvement of the as-prepared iPP composites, when the nanotube content increases: (i) the flocculated structure, which is formed by interconnected nanotubes and incorporated iPP matrix; and (ii) the homogeneity of the composites.

Thus, the maximum enhancement of the tensile strength and modulus of iPP/MWCNT composites is observed around the rheological flocculation threshold of 0.5 wt % MWCNT. Although, the increase of the nanotube content above this critical concentration, produces a strong decrease of the relative tensile characteristics, probably due to the worsening of homogeneity of the nanotube dispersions. The homogeneous distribution of the floccules

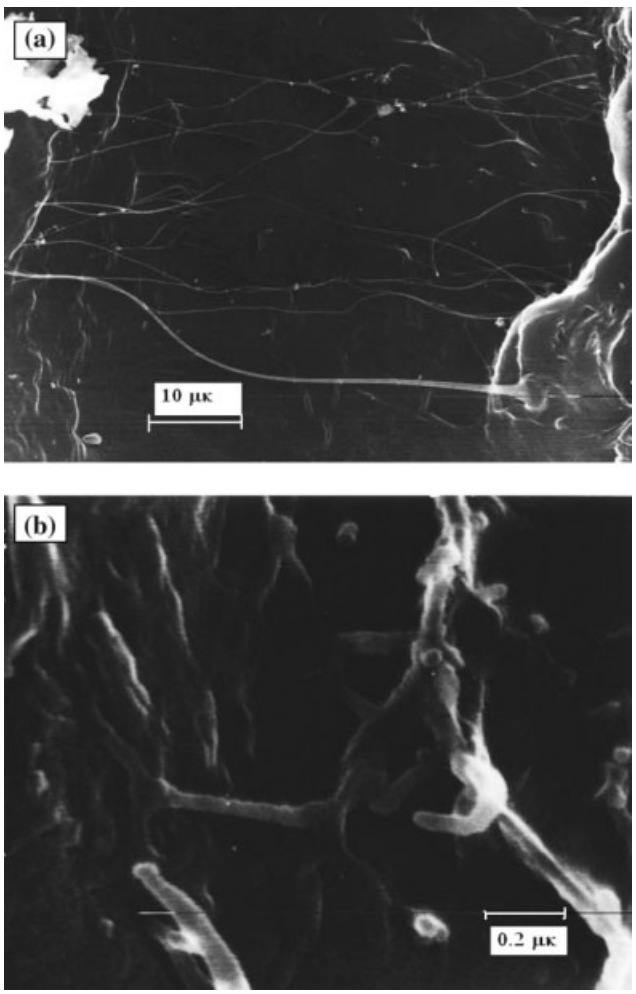

Figure 9 SEM micrographs of nanocomposites visualizing the CNT bridging a matrix crack: (a) iPP/1% MWCNT composites with magnification 10 μm and (b) iPP/0.1% MWCNT with magnification (0.2 μm).

around φ* is found reasonable for reaching maximum enhancement in mechanical properties.

In general, the iPP/MWCNT nanocomposites are thermally much more stable than iPP and this effect becomes visible above the rheological flocculation concentration of nanotubes. For example, the addition of 1%–3% nanotubes has shifted the TGA curves of iPP by 23°C–81°C toward higher temperatures in nitrogen and air atmospheres. The network structure of interconnected nanotubes and the physically absorbed iPP molecules on the nanotube surface results in enhanced thermal stability, as in these conditions the iPP molecules are much less active than those in the pure iPP and their volatilization is delayed.

The addition of nanotubes significantly increases the nanocomposite stiffness, and this effect is more pronounced at concentrations above the flocculation threshold. Thus, 3% MWCNT additive produces ~30% increase of the dynamic storage modulus. The DMTA results confirm that the MWCNT additive slightly enhances the local dynamics of iPP molecules in the glass transition region and suppresses the global relaxation of the chain segments in the amorphous regions, resulting in a reinforcement effect.

The positive influence of the CNT on the fracture mechanism is attributed to the hierarchy of the flocculated nanocomposite morphology and to bridging a matrix crack by the nanotube fibrils oriented perpendicularly to the crack front.

References

1. Thostenson, E. T.; Chou, T. W. J Phys D 2003, 36, 573.
2. Ci, L.; Ba, J. B. Composite Sci Technol 2006, 66, 599.
3. Kashiwagi, T.; Grulk, E.; Hilding, J.; Groth, K.; Harris, R.; Butler, K. Polymer 2004, 45, 4227.
4. Yang, J.; Lin, Y.; Wang, J.; Lai, M.; Li, J.; Liu, J.; Tong, X.; Cheng, H. J Appl Polym Sci 2005, 98, 1087.
5. Yu, M. F.; Lourie, O.; Dyer, M. J.; Moloni, K.; Kelly, T. F.; Rouff, R. S. Science 2000, 287, 637.
6. Li, C.; Chou, T. W. Composite Sci Technol 2003, 63, 1517.
7. Iijima, S. Nature 1991, 354, 56.
8. Fielder, B.; Gojny, F.; Wichmann, M. H. G.; Nolte, M. C. M.; Schulte, K. Compos Sci Tech 2005, 66, 3115.
9. Kotsilkova, R.thermosetting Nanocomoposites for Engineering Application; Rapra Smiths Group: United Kingdom, 2007.
10. Kotsilkova, R.; Fragiadakis, D.; Pissis, P. J Polym Sci Part B: Polym Phys 2005, 43, 522.
11. Kotsilkova, R. J Appl Polym Sci 2005, 97, 2499.
12. Funck, A.; Kaminsky, W. Composite Sci Technol 2007, 67, 906.
13. Lee, G. W.; Jagannathan, S.; Chae, H. G.; Minus, M. L.; Kumar, S. Polymer 2008, 49, 1831.
14. Valentini, L.; Biagioti, J.; Kenny, J. M.; Manchado, M. A. L. J Appl Polym Sci 2003, 89, 2657.
15. Kearns, J. C.; Shamibaugh, R. L. J Appl Polym Sci 2002, 86, 2079.
16. Zhao, P.; Wang, K.; Yang, H.; Zhang, Q.; Du, R.; Fu, Q. Polymer 2007, 48, 5688.
17. Silvestre, C.; Chimmino, S.; Raimo, M.; Carfagna, C.; Vapuano, V.; Kotsilkova, R. Macromol Symp 2005, 228, 99.
18. Madorsky, S. L.Thermal Degradation of Organic Polymers; Interscience Publication: New York, 1964.
19. Zanetti, M.; Camino, G.; Reichert, P.; Mulhaupt, R. Macromol Rapid Commun 2001, 22, 176.
20. Andrews, R.; Jacques, D.; Quia, D.; Dickey, E. C. Carbon 2001, 39, 1681.
21. Bom, D.; Andrews, R.; Jacques, D.; Anthony, B.; Chen, B.; Meier, M. S.; Selegue, J. P. Nano Lett 2002, 2, 615.
22. Mccrum, N. G.; Read, B. E.; Williams, G.Anelastic and Dielectric Effects in Polymeric Solids; John Wiley and Sons: London, New York, 1967.
23. Bershtein, V. A.; Egorova, L. M.; Yakushev, P. N.; Pissis, P.; Sysel, P.; Brozova, L. J Polym Sci Part B: Polym Phys 2002, 40, 1056.
24. Pissis, P. In Thermosetting Nanocomposites for Engineering Applications; Kotsilkova, R., Ed.; Rapra Smiths Group: United Kingdom, 2007.
25. Lima, M. F. S.; Vasconcellos, M. A. Z.; Samios, D. J Polym Sci Part B: Polym Phys 2002, 4, 896.